ChemComm

# 2H → 1T Transition and Hydrogen Evolution Activity of MoS2, MoSe2, WS2 and WSe2 Strongly Depends on the MX2 composition

SCHOLARONE™
Manuscripts

**ARTICLE TYPE**

# 2H → 1T Phase Transition and Hydrogen Evolution Activity of MoS$_2$, MoSe$_2$, WS$_2$ and WSe$_2$ Strongly Depends on the MX$_2$ composition

Adriano Ambrosi, Zdeněk Sofer and Martin Pumera*

Abstract: **We investigate here the four most widely considered TMD materials: MoS$_2$, MoSe$_2$, WS$_2$ and WSe$_2$. A 2H→1T phase transition occurs during the chemical exfoliation with different efficiencies among the four**
10 **materials.**

Transition metal dichalcogenides (TMDs) have recently attracted enormous attention by the scientific community due to their layered structure similar to graphite and their interesting
15 properties that emerge when the materials are down-sized to single or few layers.[1-3] The advantages of TMD materials versus graphene are mostly related to the fact that several properties, in particular band-gap dependent electronic properties, can be tuned by changing the metal/chalcogen composition with an array of
20 possibilities ranging from the semiconductor MoS$_2$ with large band gap of ~2 eV to the superconducting PdTe$_2$.[1] In addition to their applications in electronics, TMDs possess interesting catalytic properties for electrochemically-assisted production of hydrogen (HE), which can promote efficient and low-cost
25 production of hydrogen without the use of precious Pt-based catalysts.[4-6] Such characteristics have ignited extensive research aiming at understanding the catalytic mechanism and consequently the synthesis of TMDs with different morphologies for improved performances. Recent theoretical studies have
30 revealed the key role played by the sulfur-terminated edges of MoS$_2$ as the active site for the reaction.[7,8] Edge-sites have demonstrated superior catalytic and electrochemical activity not only for MoS$_2$ but also for other TMDs such as MoSe$_2$, WS$_2$ and WSe$_2$.[9,10] One of the methods to enhance the catalytic properties
35 is therefore to fabricate TMDs with increased edge-exposed surface with respect to the basal portion, as recently proposed.[9,11] Another key factor influencing the catalytic properties of the TMD materials is their electrical conductivity which facilitates good communication between the electron source and the active
40 edge sites.[12] Layered TMD materials present generally two different polymorph structures depending on the metal coordination by the six chalcogen atoms. In the 2H structure the metal atom coordination is trigonal prismatic and the material is semiconducting. In the 1T structure the metal coordination is
45 trigonal antiprismatic (or octahedral) inferring to the material a metal character. Li intercalation with organolithium compounds

has been proposed almost three decades ago to split apart the layers of bulk TMD materials in order to obtain single or few layer sheets[13-15] and it is still very commonly employed to
50 enhance their optical, electronic and catalytic properties.[16-18] Particularly for the catalytic properties, it has been shown that the enhanced activity not only stemmed from the reduced sheet size and increased edge-exposed surface, but also because the exfoliation process induces a phase transition between the natural
55 semiconducting 2H phase to the metallic 1T phase and therefore facilitating the electron transfer from electrode to the active edges.[12,17,19,20] It is worth noticing that a large portion of scientific works are focused on understanding and/or improving the catalytic activity of MoS$_2$ and WS$_2$ materials. As such, the
60 properties of other TMDs such as WSe$_2$ and MoSe$_2$ towards the HE reaction are almost unexplored. Interestingly, there is rarely a comprehensive side-by-side comparison of different TMDs in the literature aiming at understanding the influence of metal/chalcogen composition on the catalytic properties.
65 Here, we exfoliate four TMD materials (MoS$_2$, MoSe$_2$, WS$_2$, WSe$_2$) by a similar method (using *tert*-butyllithium intercalant; *t*-BuLi) which thus allows a direct side-by-side comparison of their performances for HER. Given the intrinsic catalytic properties of each TMD material in their bulk state, we show that the Li
70 intercalation process with *t*-BuLi produces, as expected, improved catalytic properties for all materials but with significantly different magnitudes. Based on high-resolution TEM (HR-TEM), X-ray photoelectron spectroscopy (XPS), Raman spectroscopy and electrochemical methods, we show that
75 the different catalytic properties can be linked to the efficiency of the 2H→1T transition of the materials upon intercalation. WS$_2$ and MoSe$_2$ were converted more efficiently from the natural 2H semiconducting form to the metallic 1T form compared to MoS$_2$ and WSe$_2$. In fact, WS$_2$ and MoSe$_2$ achieved the best catalytic
80 performances for the HE reaction.

Four natural transition metal dichalcogenides (TMDs), i.e. MoS$_2$, MoSe$_2$, WS$_2$ and WSe$_2$ were chemically exfoliated using Li intercalation method. Instead of using the generally adopted *n*-butyllithium (*n*-BuLi), we employed *tert*-butyllithium (*t*-BuLi) as
85 the organolithium intercalant which demonstrated equal, if not superior intercalation abilities than the former.[21] The four exfoliated materials have been fully characterized by HR-TEM,

XPS, Raman spectroscopy and electrochemically tested as catalyst for hydrogen evolution. Figure 1 shows representative high-resolution TEM images of the four TMDs. Figure 1A shows a single layer $MoS_2$ sheet characterized by a clearly visible crystalline order with however different domains. These may indicate the coexistence of both 2H and 1T phase. Multilayer structures were also visible (Figure 1B) with interlayer distances of 0.65 nm. $MoSe_2$ presented even more crystal disorder compared to $MoS_2$ where the atomic distances could hardly be measured (Figure 1C). The multilayer portions revealed a separation of about 0.6 nm (Figure 1D). Similar aspect was shown by $WS_2$ (Figure 1E) which presented disordered crystal domains. Single layer was hardly detected for $WS_2$ and the distance of adjacent layers was also close to 0.6 nm (Figure 1F). Despite a very homogeneous and continuous crystal domain as seen in Figure 1G, $WSe_2$ sheet contained different polymorphs on the same layer. A closer look at the image (see inset Figure 1G) revealed portions with hexagonal structures which are typically seen for the 1T phase and also honeycomb lattices characteristic of the 2H phase.[22] The interlayer distances were measured to be around 0.65 nm (Figure 1H) for multilayer structure of the material. In general, it can be concluded from the TEM analysis that the exfoliation was more efficient on $MoS_2$ and $MoSe_2$ given the high presence of single-to-few layer structures. $WS_2$ and $WSe_2$ were also exfoliated but consisted of few-to-several layer structures. As for the crystal phase, the TEM images suggested the presence of different domains within the same TMD layer, indicating the existence of both the 1T and 2H polymorphs. Low-resolution TEM images of the exfoliated TMD materials are presented in Figure **S1** of Supporting information. We next moved on with the characterization using Raman spectroscopy to obtain further information on the structure and the number of layers for the exfoliated TMDs. Raman spectra of the four exfoliated TMD materials are shown in Figure S3 of Supporting Information. $MoS_2$ (Figure S3A) consisted of the well-known in-plane $E^1_{2g}$ and out-of-plane $A_{1g}$ modes at 380 and 405 $cm^{-1}$, respectively. The separation between the two modes (~25 $cm^{-1}$) would suggest a multilayer structure according to recent studies.[23] However, the softening of both modes in comparison with the signal recorded for the bulk $MoS_2$ starting material indicated a reduced number of layers as well as a reduced lateral size (Figure S2A).[21,24] Similar to $MoS_2$, the Raman spectrum of $WS_2$ (Figure S3C) which showed the in-plane $E^1_{2g}$ and out-of-plane $A_{1g}$ modes at about 350 and 417 $cm^{-1}$, respectively were also softened with respect to the bulk material (Figure S2C). $MoSe_2$ (Figure S3B) comprised of an $A_{1g}$ mode at about 237 $cm^{-1}$, which was red-shifted and softened as compared to the bulk material(Figure S2B) indicating the presence of single or few layer structures.[25] A single band observed on $WSe_2$ (Figure S3D) at about 249 $cm^{-1}$ was assigned to the $A_{1g}$ vibration mode. Again, its softening with respect to the band recorded for the bulk material (Figure S2D) can be linked to the reduced number of layers. X-ray photoelectron spectroscopy is an effective and useful tool to distinguish the 2H and 1T polymorphs of TMD materials.[16, 26] Figure 2 shows the high-resolution XPS spectra of Mo 3d and W 4f for the four TMDs materials investigated. Mo 3d signals corresponding to $Mo^{4+}$ $3d_{5/2}$ and $Mo^{4+}$ $3d_{3/2}$ of the 2H polymorph
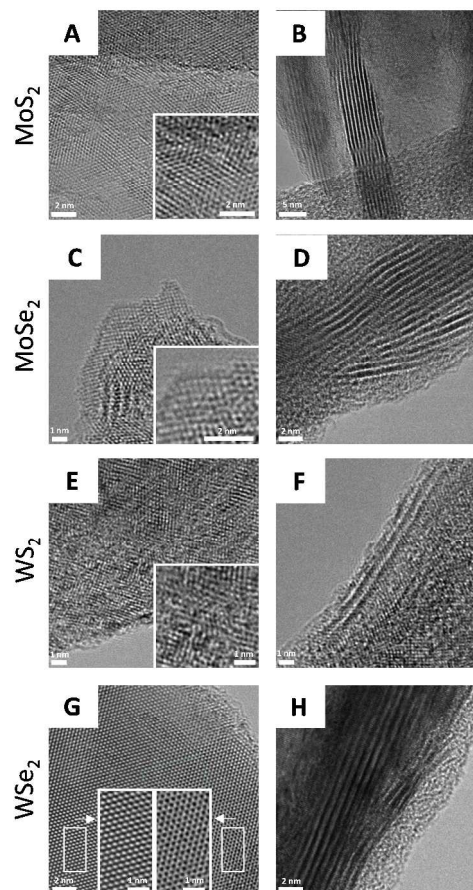


**Fig. 1** High-resolution TEM images of exfoliated $MoS_2$ (A, B), $MoSe_2$ (C, D), $WS_2$ (E, F) and $WSe_2$ (G, H). Left column: view from a direction perpendicular to the basal plane of TMD layer; right column: view from a direction parallel to TMD layer. Bottom-inset: enlarged views of basal plane in order to clearly present the crystalline structure.

were generally observed at 229 and 232 eV,[16] respectively, similar to the natural $MoS_2$ and $MoSe_2$ bulk (See Figure **S4** in Supporting Information). The presence of additional peaks at lower binding energies indicated the coexistence of the 1T form. As it can be seen in Figure 2A, $MoS_2$ consisted almost exclusively of the $Mo^{4+}$ peaks from the 2H form and with only a small portion of the 1T. On the contrary, $MoSe_2$ contained a significant contribution from the 1T phase since peaks at lower binding energies (228 and 231 eV) were detected together with those of the 2H phase (Figure 2B). This indicated that Li intercalation through $t$-BuLi was able to convert $MoSe_2$ from the 2H form to the metallic 1T form more efficiently. A signal appearing at a higher binding energy (>233 eV) corresponding to $Mo^{6+}$ suggested the formation of $MoO_3$ species. It can be seen that both the $MoS_2$ and $MoSe_2$ comprised of such oxidative signals. Considering the W 4f spectra, the signals at about 33 and 35 eV were generally attributed to the $W^{4+}$ $4f_{7/2}$ and $W^{4+}$ $4f_{5/2}$ in the natural semiconducting 2H form.[26] It can be seen that while $WSe_2$ contained almost exclusively the signals of the 2H form (Figure 2D), $WS_2$ resulted with a larger percentage of the 1T phase as indicated by the presence of peaks at about 32 and 34 eV (Figure 2C).[26] Similarly, signals at higher binding energies (>36

eV) indicated the presence of $W^{6+}$ species within the material which was most likely existing in the oxide form of $WO_3$.[26] Similar results were obtained accordingly on the S 2p and Se 3d high-resolution spectra (Figure **S5** of Supporting Information). From the XPS data, it can be concluded that Li intercalation/exfoliation of the bulk materials by means of *t*-BuLi resulted in a more efficient 2H→1T conversion for $WS_2$ and $MoSe_2$ but less efficient for $MoS_2$ and $WSe_2$. In order to further support the XPS results we performed resistivity measurements of the four materials using an interdigitated Au electrode (Au-IDE). Applying an AC voltage of 10 mV we recorded the variation of the resistivity with the potential frequency applied. Figure S9 of Supporting Information summarizes the resistivity values taken at the low frequency of 0.15 Hz. It can be seen that $MoSe_2$ and $WS_2$ resulted the materials with the lowest planar resistivity ($\approx$ 0.5 Ohm) followed by $MoS_2$ ($\approx$ 3 Ohm) and finally $WSe_2$ presenting the highest resistivity of about 65 Ohm. It is evident that the materials presenting the largest portion of the 1T phase ($WS_2$ and $MoSe_2$) resulted also the most conductive. Significant differences should thus be expected in terms of the catalytic activity of the four exfoliated materials towards HER. We then explored electrochemically-assisted hydrogen production in acidic media using GC electrodes modified with a fixed amount of the four TMDs. For a better comparison, we have included the polarization curves of the four materials in their bulk state as well as bare GC electrode and GC electrode modified with Pt/C (20% Pt on Vulcan carbon) as the standard catalytic material for this investigation. It can be observed in Figure 3 that the exfoliation procedure has improved the catalytic activities of all the TMDs for hydrogen evolution as expected from the reduced number of layers, increased conductivity of the materials and the larger surface of exposed edges. By comparing only the exfoliated materials, it can be seen $WS_2$ and $MoSe_2$ have outperformed $MoS_2$ and $WSe_2$ as they only required low overpotential of about 0.35 V (vs RHE) to generate 10 mA current. $MoS_2$ required a potential of about -0.55 V to reach the same current value while $WSe_2$ required about -0.8 V. Pt/C showed the best performance with overpotential of about 0.05 V at the same current density of 10 mA/cm$^{-2}$. Bare GC electrode demonstrated poor catalytic properties towards HE reaction since it required a much higher overpotential. For this reason, GC is an ideal platform to investigate the TMDs since it does not influence and/or interfere with the properties of the materials. Interestingly, the bulk $MoS_2$, $WS_2$ and $WSe_2$ presented similar catalytic properties with overpotential of about 0.85 V while only $MoSe_2$ seemed to have a more favorable intrinsic catalytic ability to generate hydrogen, resulting in overpotential of about 0.65 V. Considering the three former, it was evident that despite similar intrinsic catalytic properties, their performances differed significantly after the exfoliation with *t*-BuLi. $WS_2$ experienced the most impressive improvement upon exfoliation (Figure 3B), with an overpotential shift of about 500 mV. $MoS_2$ (Figure 3A) resulted with an overpotential shift of about 300 mV and $WSe_2$ of only 50-100 mV (Figure 3D). $MoSe_2$ showed an overpotential shift of about 300 mV (Figure 3C), which ultimately turned it into the best performing material due to its more favorable intrinsic catalytic properties.
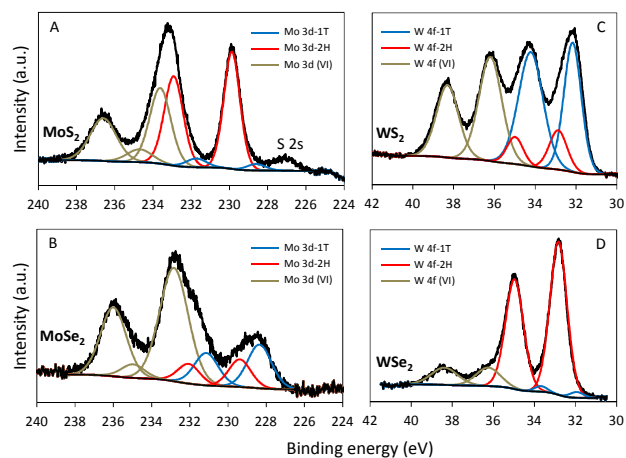


**Fig. 2** High-resolution XPS spectra of Mo 3d (left) and W 4f (right) in exfoliated (A) $MoS_2$, (B) $MoSe_2$, (C) $WS_2$ and (D) $WSe_2$.

Closer analyses of these results indicated a very good correlation between the catalytic performances of the four exfoliated materials with the presence of 1T phase as determined by XPS (Figure 2). $WS_2$ and $MoSe_2$ which gave the best performance for hydrogen evolution reaction were, in fact, the materials with the largest composition of 1T phase. Such a transition of 2H→1T is therefore much more favorable on $WS_2$ and $MoSe_2$ as compared to $MoS_2$ and $WSe_2$, despite the employment of a common Li intercalation/exfoliation procedure with *t*-BuLi. Tafel plots can be used to evaluate the mechanism involved in the HE reaction. In particular, when the slope (*b*) of the linear portion of the plot is about 30 mV/decade, the HE reaction follows the so-called Volmer-Tafel mechanism. This is typical for Pt catalyst as confirmed in our results (see Figure S10 of Supporting Information). When the hydrogen adsorption represents the rate determining step, the Tafel slope is about 120 mV/decade and the HER follows the so-called Volmer mechanism. Tafel slope for the investigated TMD materials resulted >240 mV/decade for $WSe_2$ confirming the poor catalytic performance of this material. $MoS_2$ resulted with a slope of about 99 mV/decade which is similar to previous results.[21] The lowest Tafel slopes were obtained for $WS_2$ and $MoSe_2$ giving values of 85 and 82 mV/decade, respectively. This confirms the superior performance of these two materials compared to the others as shown also in the polarization curves in Figure 3. Having a Tafel slope values which fall between the Volmer mechanism (*b* = 120 mV/decade) and the Heyrovsky mechanism (*b* = 40 mV/decade), a combined (Volmer-Heyrovsky) mechanism is expected where both reactions influence the HER rate. This side-by-side comparison of the four most representative TMD materials ($MoS_2$, $MoSe_2$, $WS_2$ and $WSe_2$) reveals that the effectiveness of chemical exfoliation through Li intercalation is different depending on the TMD materials employed. In fact, it is particularly effective for $WS_2$ which demonstrated impressive catalytic performances for HE. It is worth noting that even though the 2H→1T transition accompanying the Li intercalation of bulk $MoSe_2$ is less efficient, such material can offer an equally impressive catalytic performance. This is due to the intrinsic catalytic properties of $MoSe_2$ even in its natural bulk state which is superior to the other

TMDs. A more efficient exfoliation with consequent 2H→1T transition should therefore represent the focus of future works particularly for MoSe₂, which is potentially the most promising material for electrocatalytic hydrogen production.
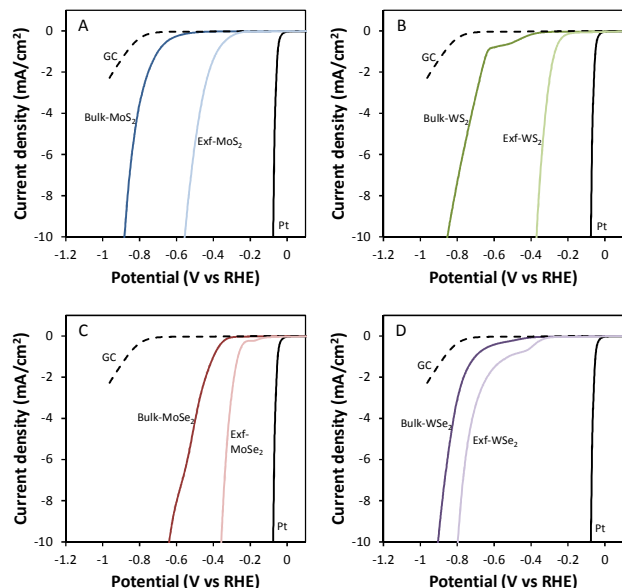


**Fig. 4** Polarization curves obtained with bulk and exfoliated TMD materials in 0.5 M H₂SO₄. (A) MoS₂, (B) WS₂, (C) MoSe₂ and (D) WSe₂.

A side-by-side comparison of the four most representative TMD materials MoS₂, MoSe₂, WS₂, WSe₂ has been carried out in relation to their catalytic properties towards hydrogen evolution (HE) reaction. We employed a common chemical procedure via Li intercalation using *t*-BuLi organolithium compound to exfoliate the four materials at their natural bulk state. Using HR-TEM, Raman spectroscopy, XPS and voltammetry we showed that the efficiencies of Li intercalation and exfoliation are contrastingly different for the four materials and which consequently generates different performances for HE. We show that the different catalytic properties offered by the exfoliated materials can be linked to the portion of the materials existing in the 1T phase. The transition of 2H→1T is, in fact, more efficient for WS₂ and MoSe₂ resulting in a larger composition of 1T phase compared to WSe₂ and MoS₂. WS₂ and MoSe₂ were the best performing catalysts for HE as they required overpotential of as little as 0.35 V to generate 10 mA current. Despite such similar performances offered by WS₂ and MoSe₂, the portion of 1T phase was larger for the former. Therefore, MoSe₂ is potentially the most promising material as catalyst if a more efficient exfoliation and consequently a larger portion of metallic 1T phase is produced. These results show the importance of a direct side-by-side comparison of several materials which is rarely available in the literature. A comparative study is particularly important in search for highly efficient catalysts for HE as well to provide insight into the underlying electrochemical activity of TMDs.

## Acknowledgement

## Notes and references

*Division of Chemistry & Biological Chemistry, School of Physical and Mathematical Sciences, Nanyang Technological University, Singapore 637371, Singapore. Fax: (65) 67911961. Email: pumera@ntu.edu.sg*

1.  M. Chhowalla, H. S. Shin, G. Eda, L.-J. Li, K. P. Loh and H. Zhang, *Nat. Chem.*, 2013, **5**, 263.
2.  M. Xu, T. Liang, M. Shi and H. Chen, *Chem. Rev.*, 2013, **113**, 3766.
3.  M. Pumera, Z. Sofer and A. Ambrosi, *J. Mater. Chem. A*, 2014, **2**, 8981.
4.  J. R. McKone, S. C. Marinescu, B. S. Brunschwig, J. R. Winkler and H. B. Gray, *Chem. Sci.*, 2014, **5**, 865.
5.  J. D. Holladay, J. Hu, D. L. King and Y. Wang, *Catal. Today*, 2009, **139**, 244.
6.  A. B. Laursen, S. Kegnaes, S. Dahl and I. Chorkendorff, *Energy Environ. Sci.*, 2012, **5**, 5577.
7.  T. F. Jaramillo, K. P. Jørgensen, J. Bonde, J. H. Nielsen, S. Horch and I. Chorkendorff, *Science*, 2007, **317**, 100.
8.  J. Kibsgaard, Z. Chen, B. N. Reinecke and T. F. Jaramillo, *Nat. Mater.*, 2012, **11**, 963.
9.  D. Kong, H. Wang, J. J. Cha, M. Pasta, K. J. Koski, J. Yao and Y. Cui, *Nano Lett.*, 2013, **13**, 1341.
10. C. Tsai, K. Chan, F. Abild-Pedersen and J. K. Norskov, *Phys. Chem. Chem. Phys.*, 2014, **16**, 13156.
11. D. Y. Chung, S. K. Park, Y. H. Chung, S. H. Yu, D. H. Lim, N. Jung, H. C. Ham, H. Y. Park, Y. Piao, S. J. Yoo and Y. E. Sung, *Nanoscale*, 2014, **6**, 2131.
12. Y. Li, H. Wang, L. Xie, Y. Liang, G. Hong and H. Dai, *J. Am. Chem. Soc.*, 2011, **133**, 7296.
13. P. Joensen, R. F. Frindt and S. R. Morrison, *Materials Research Bulletin*, 1986, **21**, 457.
14. M. Kertesz and R. Hoffmann, *J. Am. Chem. Soc.*, 1984, **106**, 3453.
15. W. M. R. Divigalpitiya, S. R. Morrison and R. F. Frindt, *Thin Solid Films*, 1990, **186**, 177.
16. G. Eda, H. Yamaguchi, D. Voiry, T. Fujita, M. Chen and M. Chhowalla, *Nano Lett.*, 2011, **11**, 5111.
17. D. Voiry, M. Salehi, R. Silva, T. Fujita, M. W. Chen, T. Asefa, V. B. Shenoy, G. Eda and M. Chhowalla, *Nano Lett.*, 2013, **13**, 6222.
18. H. Wang, Z. Lu, S. Xu, D. Kong, J. J. Cha, G. Zheng, P.-C. Hsu, K. Yan, D. Bradshaw, F. B. Prinz and Y. Cui, *Proc. Natl. Acad. Sci. USA*, 2013, **110**, 19701.
19. M. A. Lukowski, A. S. Daniel, F. Meng, A. Forticaux, L. S. Li and S. Jin, *J. Am. Chem. Soc.*, 2013, **135**, 10274.
20. D. Voiry, H. Yamaguchi, J. Li, R. Silva, D. C. B. Alves, T. Fujita, M. Chen, T. Asefa, V. B. Shenoy, G. Eda and M. Chhowalla, *Nat. Mater.*, 2013, **12**, 850.
21. A. Ambrosi, Z. Sofer and M. Pumera, *Small*, 2014, n/a.
22. G. Eda, T. Fujita, H. Yamaguchi, D. Voiry, M. Chen and M. Chhowalla, *ACS Nano*, 2012, **6**, 7311.
23. H. Li, Q. Zhang, C. C. R. Yap, B. K. Tay, T. H. T. Edwin, A. Olivier and D. Baillargeat, *Adv. Funct. Mater.*, 2012, **22**, 1385.
24. H. S. S. Ramakrishna Matte, A. Gomathi, A. K. Manna, D. J. Late, R. Datta, S. K. Pati and C. N. R. Rao, *Angew. Chem. Int. Ed.*, 2010, **49**, 4059.
25. P. Tonndorf, R. Schmidt, P. Böttger, X. Zhang, J. Börner, A. Liebig, M. Albrecht, C. Kloc, O. Gordan, D. R. T. Zahn, S. Michaelis de Vasconcellos and R. Bratschitsch, *Optics Express*, 2013, **21**, 4908.
26. B. Mahler, V. Hoepfner, K. Liao and G. A. Ozin, *J. Am. Chem. Soc.*, 2014, **136**, 14121.